Langmuir

Article

pubs.acs.org/Langmuir

Halide Exchange on Mg(II)−Al(III) Layered Double Hydroxides: Exploring Affinities and Electrostatic Predictive Models

Víctor Oestreicher,[†] Matías Jobbágy,*[,†,‡] and Alberto E. Regazzoni[§,∥]

[†]INQUIMAE-DQIAQF, Facultad de Ciencias Exactas y Naturales, Universidad de Buenos Aires, Ciudad Universitaria, Pabellón II, C1428EHA, Buenos Aires, Argentina

[‡]Centro Interdisciplinario de Nanociencia y Nanotecnología, Argentina

[§]Unidad de Actividad Química, Centro Atómico Constituyentes, Comisión Nacional de Energía Atómica, Avenida General Paz 1499, B1650KNA-San Martín, Argentina

[∥]Instituto de Tecnología Jorge Sábato, Universidad Nacional de General San Martín, Avenida General Paz 1499, B1650KNA-San Martín, Argentina

Supporting Information

ABSTRACT: The crystalline chloride form of layered double hydroxide (LDH) with the formula $Mg_{0.75}Al_{0.25}(OH)_2Cl_{0.25}\cdot mH_2O$ was gradually exchanged with F^-, Br^-, or I^- up to a total displacement of Cl^-. For the three anions, both the exchange isotherms as well as the structural changes were inspected along the whole range of chloride displacement. The bulkier Br^- and I^- followed an ideal exchange behavior isotherm while F^- denoted strong deviations from the ideal regime as well as phase segregation. The exchange constants recorded herein were contrasted with bibliographic data belonging to an analogous LDH host, revealing a strong linear free energy correlation. Higher Al(III) to Mg(II) ratios, or layer charge densities, favor a stronger selectivity for smaller halides. For both hosts, the exchange free energy was satisfactorily described in terms of strictly electrostatic-based models.

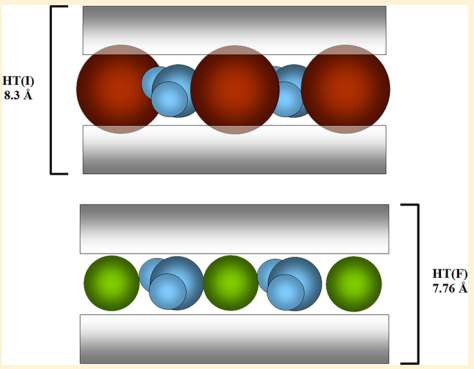

INTRODUCTION

Layered double hydroxides (LDHs), also known as anionic clays, constitute a vast family of compounds bearing the general formula $M^{II}_{1-x}M^{III}_x(OH)_2A^{z-}_{x/z} \gg nH_2O$, where x typically ranges between 0.20 and 0.33.[1] These crystalline compounds relate to the mineral phase hydrotalcite $[Mg_6Al_2(OH)_{16}(CO_3)\cdot 4H_2O]$, a natural occurring LDH in which both Mg(II) and Al(III) cations are located at the center of edge-sharing OH octahedrons that are interconnected to form two-dimensionally infinite sheets (or layers), resembling the basic hexagonal structure of brucite, $Mg(OH)_2$.[2] Since divalent cation positions are isomorphically substituted by trivalent ones, extra positive charges possessed by the latter give to the brucite-like layers a permanent positive charge governed by the fraction of cation positions occupied by M(III).[3] Anions are intercalated in the space contained between brucite-like layers (also referred as gallery or interlamellar space) to compensate for the layer's permanent positive charge. In addition, the remaining volume between the intercalated anions in each gallery is filled with water molecules. The ability of LDHs to exchange interlamellar anions gave birth to a huge variety of intercalation compounds.[4−8] In particular, Mg(II)−Al(III) LDHs, as well as their memory-bearing calcined derivatives, were revealed as promising sorbents for the removal of anionic pollutants from aqueous systems.[9−24] However, despite the increasing practical interest in anion-exchange reactions involving LDH phases, rigorous thermodynamic information on anionic exchange equilibria is indeed scanty, and it is mostly limited to the seminal work by Miyata[25] and others.[26,27] Considering anions as anhydrous moieties, it is well-accepted that for a certain pair of them, holding the same charge, the inherent affinity is higher for the smallest one. On the other hand, for a given size, the one holding the highest charge has the higher affinity. Finally, certain anions, like carbonate, that can accommodate two charges per anion in a flat one-atom-thick configuration exhibit an exceptional affinity that requires extreme conditions to drive its departure through anionic exchange.[28]

Beyond these accepted facts, the correlation of the relevant structural changes that accompany intercalation reactions with the overall stability of equilibrated partially exchanged LHDs remains poorly understood. Furthermore, many questions referring to the role of anion size, charge, and specific interactions on the affinity for the interlamellar spaces of LDHs are still open. To this aim, the present study thoroughly explores the structural changes of $Mg_{0.75}Al_{0.25}(OH)_2Cl_{0.25}\cdot mH_2O$ LDH as well as the inherent exchange affinities over a series of anion exchange reactions with the other halide anions.

Received: April 23, 2014
Revised: June 19, 2014
Published: June 25, 2014

   dx.doi.org/10.1021/la5015187 | *Langmuir* 2014, 30, 8408−8415

EXPERIMENTAL SECTION

A crystalline commercial hydrotalcite (DHT-6, Kyowa Kagaku Kogyo Co., Ltd.), $Mg_{0.75}Al_{0.25}(OH)_2(CO_3)_{0.125}{\cdot}mH_2O$, sample was transformed into the chloride form, $Mg_{0.75}Al_{0.25}(OH)_2Cl_{0.25}{\cdot}mH_2O$ or HT(Cl), according to the acid decarbonation−exchange procedure developed by Iyi et al.[29,30] Anion-exchange experiments were perform in volumetric Pyrex flasks. A measured volume of a solution of containing a known amount of potassium salt of the incoming halide (F^-, Br^-, or I^-) was added to a weighed amount of a previously equilibrated water suspension of HT(Cl), and the volume of the flask was completed with decarbonated water. The final concentration of HT(Cl) was 1 g dm^{-3}; those of KF, KBr, and KI ranged from 1×10^{-4} to 6×10^{-3}, 1×10^{-2}, and 1.2×10^{-1} mol dm^{-3}, respectively. All experiments were carried out at pH 9.30, i.e., the natural pH of hydrotalcite aqueous suspensions.[31] For this purpose, the pH of all halide solutions was adjusted to 9.3 by addition of KOH. In order to avoid carbonate contamination, all suspensions were kept under carbon dioxide-free nitrogen. These suspensions were left to equilibrate at 298 K for 1 h; equilibrium is attained within the first 20 min, as indicated by preliminary experiments.[32] After filtering through 0.22 μm pore size nitrocellulose membranes, anion content in the supernatants was assessed by ionic chromatography using a DEIONEX DX-100 equipped with an AS4A-SC column; filtrates were dried and kept in desiccators before powder X-ray diffraction (PXRD) inspection, employing a Siemens D-5000 diffractometer at 0.02° steps, 2 s counting time, 1 mm slits, and Ni-filtered Cu Kα radiation ($\lambda \cong$ 1.5406 Å) operating at 40 kV and 30 mA current. Peak analysis was performed using the Diffrac-AT 3.0 profile fitting software.

RESULT AND DISCUSSION

Structural Modifications Driven by Halide Exchange. As a first step to characterize the exchange behavior of HT(Cl), this phase was equilibrated with a set of solutions containing increasing concentrations of fluoride; an analogous set of experiments were also carried out with bromide and iodide. Representative samples of each one of the three sets were inspected by means of PXRD. On the basis of the halide content of each solid sample, we determined the halide-exchanged fraction, θ. This magnitude accounts for the molar fraction of initial chloride anions of HT(Cl) that were replaced by the incoming halide, X; partially exchanged phases will be described as $HT(Cl_{1-\theta}X_\theta)$ in the following. Figure 1 presents the evolution of PXRD patterns as a function of the exchanged fraction, θ, along the angular range corresponding to the interlamellar main 003 and 006 reflections.

For the three sets of exchange reactions, none of the partially exchanged phases evidenced extra signals between 11.5° and 21°, indicating the absence of ordered second staging phases.[29] In the case of fluoride- and bromide-driven exchange reactions, partially exchanged phases, $HT(Cl_{1-\theta}F_\theta)$ and $HT(Cl_{1-\theta}Br_\theta)$, denoted a continuous structural shift toward the fully exchanged HT(F) and HT(Br) end-members, respectively.[25,33] However, for the case of iodide exchange more complex structural features on the $HT(Cl_{1-\theta}I_\theta)$ phases are observed; practically all along the exchange range, the starting HT(Cl) phase is gradually transformed into two different expanded structures that coexist, evidenced by the split 003 and 006 peaks. Interestingly, this behavior remains noticeable even for the end member HT(I), characterized by the asymmetry of both interbasal reflections, in agreement with previous reports.[26] Then, this behavior cannot be ascribed to the segregation of $HT(Cl_{1-\theta}I_\theta)$ phases and probably obeys particular hydration behaviors.[34] The same LDH host intercalated with nitrate anions exclusively exhibited similar split signals under typical lab relative humidity conditions.[35]

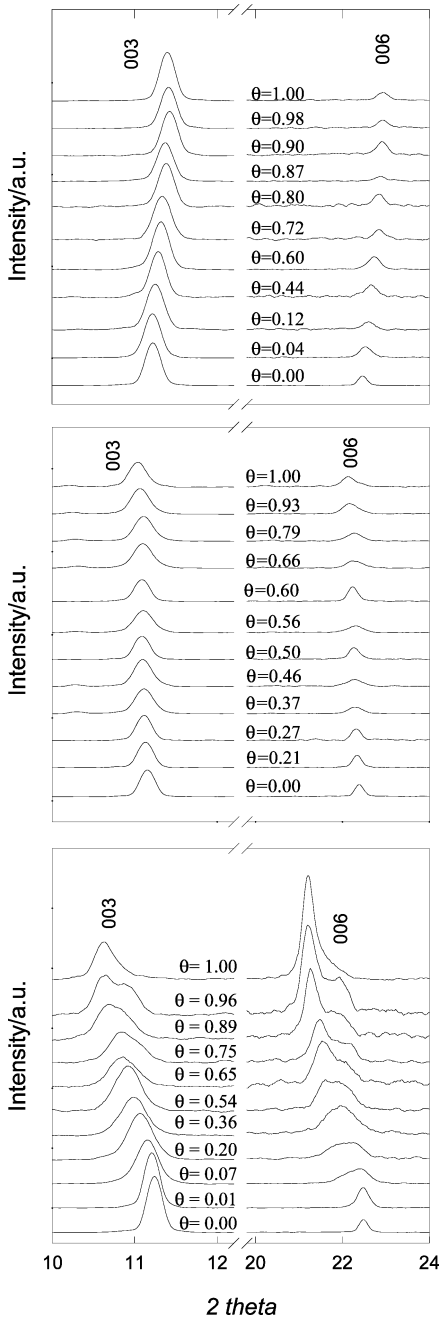

Figure 1. PXRD patterns of $HT(Cl_{1-\theta}X_\theta)$ samples obtained from HT(Cl) increasingly exchanged with fluoride (upper panel), bromide (middle panel), and iodide (lower panel).

Additionally, the coexistence of two segregated $HT(Cl_{1-\theta}I_\theta)$ phases with fixed iodide to chloride ratios was disregarded due to the lack of constancy in the value of each one of the interlamellar reflections. In these kinds of solids, the relative intensity of the 003 reflection with respect to the 006 one is governed by the interlayer scattering factor that depends on the average anion's electron density. This value remained similar for both set of signals (data not shown) as a function of θ, suggesting that both signals correspond to a single iodide to chloride stoichiometry, say a single $HT(Cl_{1-\theta}I_\theta)$ phase.[36,37] Figure 2 depicts the dependence of interlamellar distance with the exchange fraction for the three sets. Both $HT(Cl_{1-\theta}I_\theta)$ and $HT(Cl_{1-\theta}Br_\theta)$ phases reveal a continuous expansion, almost

dx.doi.org/10.1021/la5015187 | Langmuir 2014, 30, 8408−8415

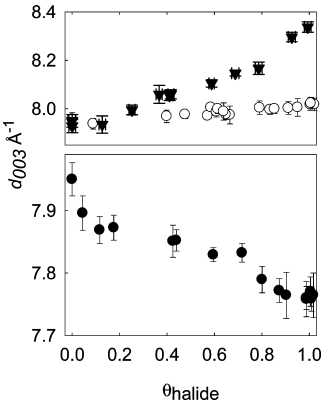

Figure 2. Interlamellar distance of HT($Cl_{1-\theta}X_\theta$) samples as a function of fluoride (●), bromide (○), or iodide (▼) exchange fractions.

linear, suggesting a Vegard-like behavior. However, HT-($Cl_{1-\theta}F_\theta$) phase, even when it continuously contracts with increasing fluoride uptake, deviates from the aforementioned linear trend. Three zones along the exchange, each one of them characterized by an almost linear trend with an inherent slope, can be identified. Samples belonging to the longest interval, bearing an overall composition in the range $0.15(5) \leq \theta \leq 0.75(5)$ evidenced the smallest structural modification.

Halide Exchange Isotherms. As the counterpart of the structural inspection, the three sets of exchange reactions were monitored in terms of solution composition. Figure 3 depicts

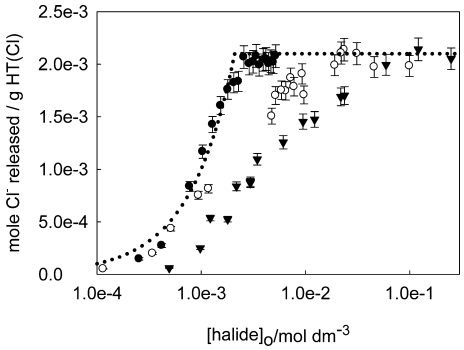

Figure 3. Mole of chloride released from a suspension containing 1 g of HT(Cl) per dm^3, as a function of the initial concentration of fluoride (●), bromide (○), or iodide (▼). Dotted line depicts the expected chloride release for a quantitative exchange reaction.

the exchange isotherms expressed as the amount of chloride released to solution as a function of the initial halide concentration. For the three sets of exchange reactions explored herein, a total removal of chloride (quantitative exchange) from the parent HT(Cl) phase was confirmed, reaching a value of 2.2×10^{-3} mol of chloride released per gram of HT(Cl) added, in excellent agreement with the chemical composition of this phase. Once these isotherms are contrasted with the limit exchange behavior imposed by a quantitative exchange reaction, depicted as a dotted line, the three sets denote clear differences in terms of the inherent affinity of each halide anion for the HT(Cl) phase. Fluoride anions displaced chloride ones with the highest affinity for HT phase, almost following the reference quantitative exchange isotherm, while iodine affinity is the lowest; the behavoir of bromide stands intermediate.

Previous experiences revealed that exchange isotherms offer reliable information concerning exchange equilibrium,[32] even for the chloride displacement by bulkier anions than the present ones. Then, the following thermodynamic analysis assumes the condition of microreversibility.

In order to assess the inherent affinity of each anion for the HT phase, the measured isotherms will be described in terms of solid-solution exchange constant formalism, traditionally employed to describe cationic exchange on clays.[38] For the studied reactions, the replacement of chloride anions intercalated within the HT phase for a given halide, X^-, is expressed by the equilibrium in eq 1:

$$X^-_{aq} + HT(Cl)_s \leftrightarrow Cl^-_{aq} + HT(X)_s \quad (1)$$

The exchange constant, $K_{X\text{-}Cl}$, relates to the activities of the involved anions, both in solution and the solid phase through eq 2. In the latter case, the activity of X^- is defined as the molar fraction of anionic sites occupied by this anion, θ_X, corrected by an activity coefficient f_X.

$$K_{X-Cl} = (f_X \theta_X a_{Cl}[Cl^-])/(f_{Cl}\theta_{Cl} a_X[X^-]) \quad (2)$$

Due to the electroneutrality, the sum of anionic fractions in the solid equals 1.

$$1 = \theta_X + \theta_{Cl} \quad (3)$$

The obtained experimental data reflects an apparent exchange constant, $Q_{X\text{-}Cl}$, defined by the concentrations quotient, instead of the activities one.

$$Q_{X-Cl} = \theta_X[Cl^-]\theta_{Cl}{}^{-1}[X^-]^{-1} \quad (4)$$

Typically, the dependence of the apparent constant with the exchanged fraction is presented in the form of the so-called Kielland plot, which clearly warns about nonideal exchange behavior, while this representation remains silent to the eventual occurrence of phase segregation.[32] The latter limitation can be overcame following the evolution of the solid's composition (exchange degree or θ) as a function of the solution's composition by means of a robust thermodynamic variable, such as the ratio between the involved anion's activities. Assuming that the activity coefficients in solution, a, for both chloride and the incoming halide are similar, the concentration ratio can be used instead of the activity one. Figure 4 depicts the evolution of exchange as a function of the incoming halide to chloride concentration ratio; both iodide

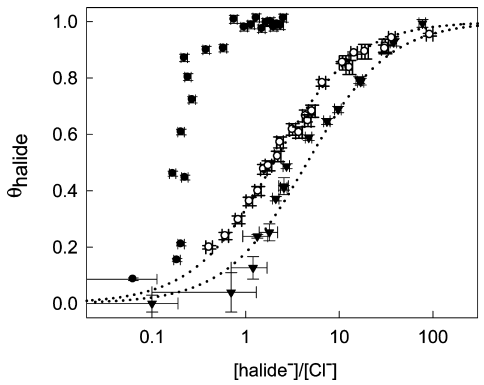

Figure 4. Halide exchange fraction, θ, as a function of chloride to fluoride (●), bromide (○), or iodide (▼) concentration ratio. Dotted lines depict fitted ideal exchange isotherms.

dx.doi.org/10.1021/la5015187 | Langmuir 2014, 30, 8408−8415

and bromide exchange isotherms can be easily interpreted in terms of a single ideal exchange isotherm, reflected as a dotted line in each case, in agreement with the Kielland representation (see Figure S1, Supporting Information). In the case of chloride−iodide exchange, the ideal behavior observed reinforces the hypothesis of the occurrence of a single HT($Cl_{1-\theta}I_\theta$) phase that experienced partial dehydration under laboratory atmosphere, before the ex situ PXRD inspection.

In contrast, fluoride−chloride exchange isotherm results in far from ideal behavior; the invariance of the $[F^-]/[Cl^-]$ ratio for HT($Cl_{1-\theta}F_\theta$) with $0.15 \leq \theta \leq 0.85$ warns about a phase segregation scenario. A previous study of the intercalation of hexacyanoferrate(III) in similar chloride-hydrotalcite let us conclude that such phenomena is correlated with the coexistence (phase segregation) of two nonpure solid phases of fixed compositions.[32] However, due to the large structural discrepancy of the involved end-members, in that case the segregation ranges are explicitly delimited by structural data. In the present case, the less defined segregation interval inferred from PXRD data limits the analysis. Then, we choose to describe the observed exchange isotherm based on a solution's behavior exclusively, following the regular solution model. In this scenario, a single parameter adjusts variable activity coefficients for the solid phase (eq 5).

$$RT \ln(f_F/f_{Cl}) = a(1 - 2\theta_F) \quad (5)$$

The optimized a coefficient equal to 2.2(1) predicts phase segregation between $0.20(5) \leq \theta_F \leq 0.80(5)$, in good agreement with structural evidence; Figure 5 depicts the optimized isotherm as well as the segregation interval.

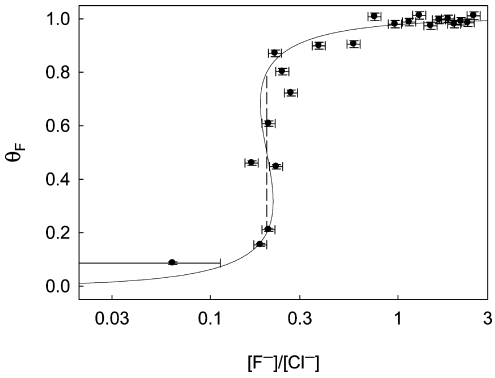

Figure 5. Fluoride−chloride exchange isotherm described in terms of the regular solution model; the vertical dashed line depicts the range predicted for phase segregation.

Under such segregation scenario, the three intervals observed for interlayer distance as a function of exchange (see Figure 2) can be reinterpreted. For the range $0 \leq \theta_F \leq 0.20(5)$, a single HT($Cl_{1-\theta}F_\theta$) phase rules the PXRD pattern. The range $0.80(5) \leq \theta_F \leq 1$ describes again a single phase, fluoride rich in this case. Along the intermediate interval, the PXRD pattern reflects a convolution of HT($Cl_{0.80(5)}F_{0.20(5)}$) and HT($Cl_{0.20(5)}F_{0.80(5)}$) segregated phases. Due to the small difference between their inherent interlayer distances, those composed patterns appear as a single 003−006 signal. This fact was corroborated by recording PXRD patterns of mechanical mixtures of the involved HT($Cl_{0.80(5)}F_{0.20(5)}$) and HT($Cl_{0.20(5)}F_{0.80(5)}$) phases.

Concerning the origin of the observed phase segregation behavior, it is worthwhile to mention that even spherical anions can occupy different and specific crystallographically sites within the interlayer space.[36,39] However, for anions bearing low electron density, their true crystallographic position remains silent to conventional PXRD inspection.[36] For a given anion, the occupancy of each kind of site depends on the LDH's water content; interlayer water departure allows a closer interaction of interlayer anions with the LDH layer, partially nesting inside the cavities left between adjacent OH groups.[40] This fact suggests that the interaction between the anion and hydrogens from water molecules and/or the LDH's OH groups controls this structural aspect. Then for a weak acid's anion such as fluoride, a stronger interaction with protons either from structural OH groups and/or interlayer water is expected, giving additional stability to certain specific arrangements of a fixed composition instead of the solid solution scenario observed for HT($Cl_{1-\theta}Br_\theta$) phases, for example.[27] The complex interplay of electrostatic forces and hydration interactions within the interlayer space is still a matter of discussion and research.[35,41−44]

Dependence of Halide Exchange Constants with LDH Composition. Beyond the observed deviations to ideal regime, the three studied reactions obey to an equilibrium constant, K_{X-Cl}, that can be obtained from the integer of the apparent constant, Q_{X-Cl}, along the whole range of exchange, according to the Gaines and Thomas formalism (see eq 6).[45]

$$\ln K_{X-Cl} = \int_0^1 \ln Q_{X-Cl}\, \partial\theta \quad (6)$$

Table 1 compiles the equilibrium constant, K_{X-Cl}, determined herein for $Mg_{0.75}Al_{0.25}(OH)_2Cl_{0.25}{\cdot}mH_2O$; data previously reported by Miyata for a parent solid phase with the formula $Mg_{0.72}Al_{0.28}(OH)_2(NO_3)_{0.25}{\cdot}mH_2O$ is presented in Table S1 (Supporting Information). In the following, the former and the latter phase will be referred to in the text as HT0.75 and HT0.72, respectively. The interlamellar distances observed for both phases totally exchanged with each one of the studied anions are also included in the correspondent tables.

Table 1. Observed Interlaminar Distances, Anionic Exchange Recorded for HT0.75

anion	d_{003} (Å)	ln K_{X-Cl}
F^-	7.76	1.73
Cl^-	7.95	
Br^-	8.05	−0.69
I^-	8.30	−1.21

For a given anion, it is well-accepted that the higher the charge and/or lower the size, the stronger the affinity for the LDH phase.[46] In the seminal work of Miyata, a linear correlation was found between the interlayer distance of each fully exchanged HT(X) phase and the standard Gibbs energy of the correspondent exchange reaction displacing the parent nitrate. More recently, ab initio simulations confirmed this tendency.[27] However, a predictive model describing the exchange affinity as a function of the inherent properties of the involved anions is still lacking. In order to compare the aforementioned data with the present one, halide-to-halide exchange equilibrium constants for HT0.72 host were inferred by combining the reported ones. Once exchange free energies belonging to each exchange pair observed on HT0.72 host are plotted against the values observed for HT0.75, a strong

dx.doi.org/10.1021/la5015187 | Langmuir 2014, 30, 8408−8415

correlation between both set of exchange reactions can be established (see Figure 6). This behavior indicates that the

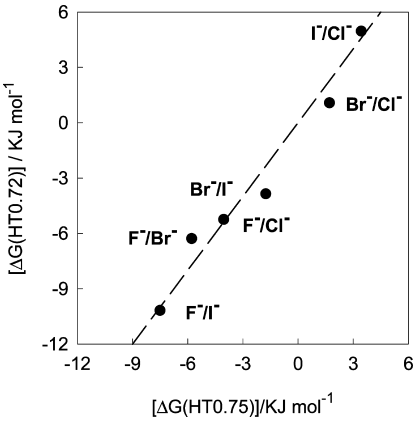

Figure 6. Correlation of the free energy of halide−halide exchange reactions recorded over HT0.72 (ref 25) and HT0.75 (present work) LDH hosts.

LDH's Mg(II) to Al(III) ratio, which governs the charge density, proportionally affects the free energy of a given anionic exchange process; certain general thermochemical stability models based on mechanical mixtures of parent single hydroxides suggest this trend.[47]

Electrostatic Models To Predict Halide Exchange Reaction Free Energy. In the following, a first microscopic attempt to understand the observed results as well as the inferred ones will be analyzed in terms of the simplest ionic exchange model, originally developed by Barrer and Townsend,[48,49] for cationic exchange reactions developed by clays (see detailed equations in the Supporting Information). The model is based on a strictly electrostatic approach in which the free energy of exchange can be estimated as the energy involved in displacing the involved ions from their initial phases, solvent and solid host, both defined as isotropic dielectrics with intrinsic permittivity ε_{Sol} and ε_{HT}, respectively, according to eq 7:

$$\Delta G^{o} = -RT \ln K = (e^2/8\pi\varepsilon_o)[(1/r_X - 1/r_{Cl})(1/\varepsilon_{HT} - 1/\varepsilon_{Sol})] \quad (7)$$

If each one of these variables except the anion's radii are considered invariant, the free energy for exchange reactions within a given LDH phase observed for a couple of monovalent anions depends exclusively on the difference between the inverse of their radii. Then, for both HT0.72 and HT0.75 phases, most of halide-to-halide exchange reactions can be satisfactorily described in terms of Barrer and Townsend's model employing Shannon's tabulated radii, water permittivity for ε_{Sol}, and an optimized value of $\varepsilon_{HT0.75} = 18$ and $\varepsilon_{HT0.72} = 14$. The magnitude of these values stand intermediate with respect to those inherent to aqueous solutions and salts; additionally, both host permittivities values are in good agreement with those obtained for related systems involving cationic exchange reactions on zeolites.[47] However, exchange reactions involving fluoride anions deviate from the halide family tendency for either HT0.72 or HT0.75 hosts. Then, in both cases, an optimized effective radius for fluoride of 1.36 Å was considered in order to overcome this deviation (see Figure 7).

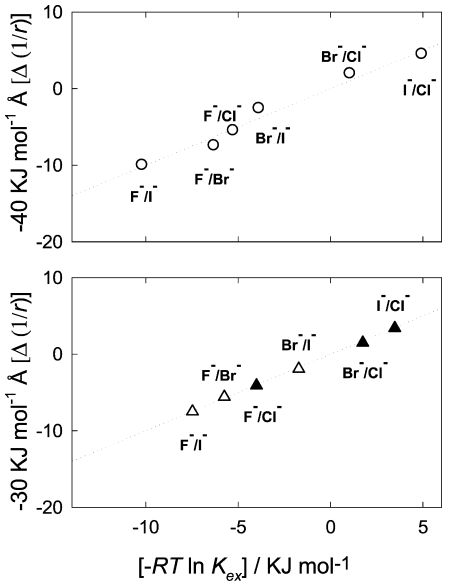

Figure 7. (Upper panel) Correlation of the experimental exchange constant and the Barrer and Townsend's model for halide−halide inferred (○) on HT0.72 host (ref 25). (Lower panel) Correlation for halide−halide observed (▲) and inferred (Δ) for HT0.75 host in the present work.

These results warn about the eventual occurrence of an effective radius that governs the intercalation process; then structural data of both HT0.72 and HT0.75 were analyzed in order to gain insight in this sense. For a given host intercalated with certain halide, the observed interlayer distance, 003, results from the sum of the layer's thickness and what we define herein the effective anionic diameter. Assuming that the former obeys to the brucitic crystallographic thickness of $Mg(OH)_2$ cell (c = 4.779 Å), the latter can be deduced. Once these effective diameters are contrasted against that of Shannon, a common linear trend can be observed for both hosts exchanged with iodide, bromide, and chloride, indicating that the bulkier the halide, the smaller the effective diameter (see Figure 8). This trend indicates partial nesting of halides inside interstitial sites delimited by three OH groups of the layer.[40] The absolute deviation is more pronounced for the HT0.72 host, due to the stronger electrostatic interaction of LDH layer bearing higher charge density. This tendency is also observed by employing

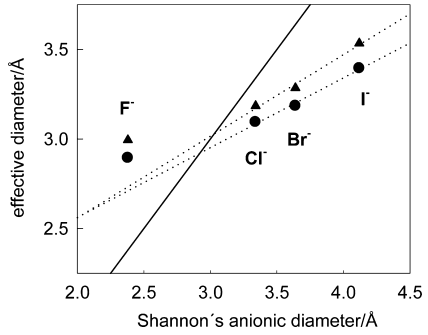

Figure 8. Correlation of the inferred effective diameter of different halides intercalated in HT0.72 (ref 25, ●) and HT0.75 (▲) and the theoretical diameter predicted by Shannon's radii (ref 50). Full line represents the match between theoretical and observed excluding diameter. Dotted lines depict the linear correlation among halides excluding fluoride anions.

dx.doi.org/10.1021/la5015187 | Langmuir 2014, 30, 8408−8415

Pauling's diameter as well (see Figure S2, Supporting Information). However, fluoride dramatically deviates from the trend, exhibiting, instead, an expanded effective diameter. Then for HT(F) phase the interlayer distance is governed by the inherent exclusion volume of intercalated water molecules (see Scheme S1, Supporting Information), in agreement with previous studies performed with the HT(NO_3) phase.[35] This anomalous behavior explains the necessity of an optimized value for fluoride's radii under Barrer and Townsend's model.

An alternative model developed by Eisenman[51] considers both an electrostatic contribution and second one accounting for hydration changes involved in the exchange reaction (see eq 8):

$$-RT \ln K = \Delta G^{\circ} \approx \Delta E_{el} + \Delta E_{hyd} \quad (8)$$

The electrostatic contribution takes into account the distance that separates the fixed charge of the host from the exchangeable cation linked to it. If the exchange reaction is described on electrostatic terms exclusively, for a given layered host, the electrostatic contribution is defined by the average distance between the center of the interlaminar ion and the layers thickness (see eq 9).

$$\Delta E_{el} = E_L[z_L z_X/(r_X + \frac{1}{2}d_L) - z_L z_{Cl}/(r_{Cl} + \frac{1}{2}d_L)] \quad (9)$$

In line with the former model, E_L is a constant accounting for the permittivity of the space that separates the charges and d_L is the thickness of the exchanger's layer of fixed charge z_L. As was stated before, the distance between the layer and the anion's center deviates from strictly geometrical considerations, say the sum of anion's radii and half the thickness of the brucitic OH−Mg(II)−OH layer. Instead, the structural parameter d_{006} is a realistic representation of the effective distance that separates those opposite charges in the case of a LDH host (see eq 10).

$$\Delta E_{el} = E_L(z_L z_X)[(d_{006}\mathrm{HT(X)})^{-1} - (d_{006}\mathrm{HT(Cl)})^{-1}] \quad (10)$$

This structural-based description of the electrostatic-based affinity of halides is able to predict the behavior of the whole family, including fluoride, either with HT0.72 or HT0.75 hosts with no further assumptions. On Figure 9, the values that account for the term $E_L(z_L z_X)$ optimized for HT0.72 and HT0.75 hosts are presented. In contrast with the former model, moisture-driven fluctuations in d_{001} data impose an experimental error on the structural term.

Since all the studied exchange reactions involved monovalent halide anions, the term $E_L(z_L z_X)$ optimized for each host depends on E_L and z_L, exclusively. Crystallographic considerations indicate that HT0.72 and HT0.75 hosts hold a charge density of 3.5 and 3.1 e/nm^2, respectively, suggesting that the effective host's charge alone explains to a great extent the observed differences.[52,53] However, differences on the magnitude of E_L cannot be disregarded.

CONCLUSIONS

The detailed exploration of the exchange reactions involving the displacement of chloride by the other halides reveals an ideal behavior for the case of bromide and iodide, while fluoride reflected a marked nonideal one that can be rationalized in terms of the regular solutions model. Structural evidence suggests phase segregation coupled with nonideal behavior for this system, in accordance with previous reports.[32] Then, even under the simplest exchange scenario, involving symmetrical reactions with spherical anions, variations of the apparent exchange are expectable.

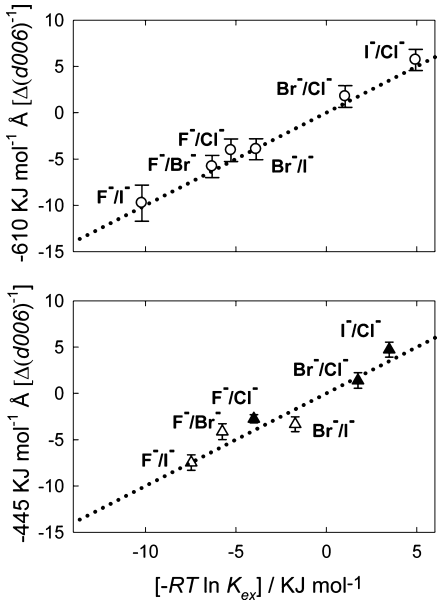

Figure 9. (Upper panel) Correlation of the experimental exchange free energy and the difference in the inverse of d_{006} for halide−halide exchange inferred (○) on phase HT0.72 (ref 25). (Lower panel) Correlation for halide−halide observed (▲) and inferred (Δ) for HT0.75 in the present work.

Experimental evidence points out that Mg(II)−Al(III) LDH host's exchange reactions are strongly dependent on Mg(II) to Al(III) ratio, which governs the layer's charge density and, hence, the ionic character of these phases. Concerning the proposed models for exchange affinities, simple electrostatic considerations have a reasonable predictive ability for spherical monovalent anions such as halides. The difference between the inverse of anionic radii arises as a suitable predictor for exchange reaction free energy, except for the case of fluoride. In such case, in which the interlayer water governs the LDH interlayer distance, the model required the optimization of an effective expanded radius. An alternative model based on the experimental LDH interlayer distance exhibited by the studied LDH phases holds a good predictive character without the necessity of the aforementioned assumption.

ASSOCIATED CONTENT

Supporting Information

Apparent exchange constants, Barrer and Townsend's model appendix, tabulated ionic radii, and scheme depicting nesting of halides. This material is available free of charge via the Internet at http://pubs.acs.org.

AUTHOR INFORMATION

Corresponding Author

*E-mail: jobbag@qi.fcen.uba.ar. Fax: 54-11-4576-3341.

Funding

This work was supported by the University of Buenos Aires (UBACyT 20020100100636), by Agencia Nacional de Promoción Científica y Tecnológica (ANPCyT PICT 2012-1167), and by National Research Council of Argentina (CONICET PIP 11220110101020).

Notes

The authors declare no competing financial interest.

■ ACKNOWLEDGMENTS

V.O. acknowledges the UBA-Estímulo and CONICET fellowship. M.J. and A.E.R. are Research Scientists of CONICET (Argentina). We are deeply indebted to Dr. N. Iyi for generously supplying the commercial hydrotalcite sample. V.O. is an honorable member of ALN.

■ REFERENCES

(1) Rives, V. *Layered Double Hydroxides: Present and Future*; Nova Publishers: New York, 2001.
(2) Evans, D. G.; Slade, R. C. T. Structural aspects of layered double hydroxides. In *Layered Double Hydroxides*; Springer: New York, 2006; Vol. *119*, pp1−87
(3) Sideris, P. J.; Nielsen, U. G.; Gan, Z. H.; Grey, C. P. Mg/Al ordering in layered double hydroxides revealed by multinuclear NMR spectroscopy. *Science* **2008**, *321*, 113−117.
(4) Rives, V.; Ulibarri, M. A. Layered double hydroxides (LDH) intercalated with metal coordination compounds and oxometalates. *Coord. Chem. Rev.* **1999**, *181*, 61−120.
(5) Newman, S. P.; Jones, W. Synthesis, characterization and applications of layered double hydroxides containing organic guests. *New J. Chem.* **1998**, *22*, 105−115.
(6) Leroux, F.; Besse, J. P. Polymer interleaved layered double hydroxide: A new emerging class of nanocomposites. *Chem. Mater.* **2001**, *13*, 3507−3515.
(7) Costantino, U.; Coletti, N.; Nocchetti, M.; Aloisi, G. G.; Elisei, F. Anion exchange of methyl orange into Zn−Al synthetic hydrotalcite and photophysical characterization of the intercalates obtained. *Langmuir* **1999**, *15*, 4454−4460.
(8) Costantino, U.; Coletti, N.; Nocchetti, M.; Aloisi, G. G.; Elisei, F.; Latterini, L. Surface uptake and intercalation of fluorescein anions into Zn−Al−hydrotalcite. Photophysical characterization of materials obtained. *Langmuir* **2000**, *16*, 10351−10358.
(9) Prasanna, S. V.; Kamath, P. V. Chromate uptake characteristics of the pristine layered double hydroxides of Mg with Al. *Solid State Sci.* **2008**, *10*, 260−266.
(10) Prasanna, S. V.; Kamath, P. V. Anion-exchange reactions of layered double hydroxides: Interplay between coulombic and H-bonding interactions. *Ind. Eng. Chem. Res.* **2009**, *48*, 6315−6320.
(11) Wang, H. T.; Chen, J.; Cai, Y. F.; Ji, J. F.; Lin, L. W.; Teng, H. H. Defluoridation of drinking water by Mg/Al hydrotalcite-like compounds and their calcined products. *Appl. Clay Sci.* **2007**, *35* (1-2), 59−66.
(12) Wang, S. L.; Liu, C. H.; Wang, M. K.; Chuang, Y. H.; Chiang, P. N. Arsenate adsorption by Mg/Al−NO_3 layered double hydroxides with varying the Mg/Al ratio. *Appl. Clay Sci.* **2009**, *43* (1), 79−85.
(13) Das, J.; Patra, B. S.; Baliarsingh, N.; Parida, K. M. Adsorption of phosphate by layered double hydroxides in aqueous solutions. *Appl. Clay Sci.* **2006**, *32* (3-4), 252−260.
(14) Das, N. N.; Konar, J.; Mohanta, M. K.; Srivastava, S. C. Adsorption of Cr(VI) and Se(IV) from their aqueous solutions onto Zr^{4+}-substituted ZnAl/MgAl-layered double hydroxides: Effect of Zr^{4+} substitution in the layer. *J. Colloid Interface Sci.* **2004**, *270* (1), 1−8.
(15) Das, J.; Patra, B. S.; Baliarsingh, N.; Parida, K. M. Calcined Mg−Fe−CO_3 LDH as an adsorbent for the removal of selenite. *J. Colloid Interface Sci.* **2007**, *316*, 216−223.
(16) Chuang, Y. H.; Tzou, Y. M.; Wang, M. K.; Liu, C. H.; Chiang, P. N. Removal of 2-chlorophenol from aqueous solution by Mg/Al layered double hydroxide (LDH) and modified LDH. *Ind. Eng. Chem. Res.* **2008**, *47* (11), 3813−3819.
(17) Chitrakar, R.; Tezuka, S.; Sonoda, A.; Sakane, K.; Ooi, K.; Hirotsu, T. Adsorption of phosphate from seawater on calcined MgMn-layered double hydroxides. *J. Colloid Interface Sci.* **2005**, *290* (1), 45−51.
(18) Jobbagy, M.; Regazzoni, A. E. Partition of non-ionic organics in hybrid-hydrotalcite/water systems. *Chem. Phys. Lett.* **2006**, *433* (1-3), 62−66.
(19) Lazaridis, N. K.; Karapantsios, T. D.; Georgantas, D. Kinetic analysis for the removal of a reactive dye from aqueous solution onto hydrotalcite by adsorption. *Water Res.* **2003**, *37* (12), 3023−3033.
(20) Lakraimi, M.; Legrouri, A.; Barroug, A.; de Roy, A.; Besse, J. P. Removal of pesticides from water by anionic clays. *J. Chim. Phys.* **1999**, *96* (3), 470−478.
(21) Bascialla, G.; Regazzoni, A. E. Immobilization of anionic dyes by intercalation into hydrotalcite. *Colloids Surf., A* **2008**, *328* (1-3), 34−39.
(22) Ookubo, A.; Ooi, K.; Tani, F.; Hayashi, H. Phase-transition of Cl-intercalated hydrotalcite-like compound during ion-exchange with phosphates. *Langmuir* **1994**, *10* (2), 407−411.
(23) Ookubo, A.; Ooi, K.; Hayashi, H. Preparation and phosphate ion-exchange properties of a hydrotalcite-like compound. *Langmuir* **1993**, *9* (5), 1418−1422.
(24) Goh, K. H.; Lim, T. T.; Dong, Z. Application of layered double hydroxides for removal of oxyanions: A review. *Water Res.* **2008**, *42* (6-7), 1343−1368.
(25) Miyata, S. Anion-exchange properties of hydrotalcite-like compounds. *Clays Clay Miner.* **1983**, *31* (4), 305−311.
(26) Israëli, Y.; Taviot-Gueho, T.; Beese, J. P.; Morel, J. P.; Morel-Desrosiers, N. Thermodynamics of anion exchange on a chloride-intercalated zinc-aluminum layered double hydroxide: A microcalorimetric study. *Dalton* **2000**, *5*, 791−796.
(27) Costa, D. G.; Rocha, A. B.; Souza, W. F.; Chiaro, S. S. X.; Leitao, A. A. Comparative structural, thermodynamic and electronic analyses of Zn−Al−A^{n-} hydrotalcite-like compounds A^{n-}=Cl^-, F^-, Br^-, OH^-, CO_3^{2-} or NO_3^-: An ab initio study. *Appl. Clay Sci.* **2012**, *56*, 16−22.
(28) Iyi, N.; Matsumoto, T.; Kaneko, Y.; Kitamura, K. Deintercalation of carbonate ions from a hydrotalcite-like compound: Enhanced decarbonation using acid−salt mixed solution. *Chem. Mater.* **2004**, *16* (15), 2926−2932.
(29) Iyi, N.; Ebina, Y.; Sasaki, T. Water-swellable MgAl−LDH (layered double hydroxide) hybrids: Synthesis, characterization, and film preparation. *Langmuir* **2008**, *24* (10), 5591−5598.
(30) Iyi, N.; Sasaki, T. Decarbonation of MgAl-LDHs (layered double hydroxides) using acetate-buffer/NaCl mixed solution. *J. Colloid Interface Sci.* **2008**, *322* (1), 237−245.
(31) Jobbágy, M.; Regazzoni, A. E. Dissolution of nano-size Mg−Al−Cl hydrotalcite in aqueous media. *Appl. Clay Sci.* **2011**, *51* (3), 366−369.
(32) Jobbágy, M.; Regazzoni, A. E. Anion-exchange equilibrium and phase segregation in hydrotalcite systems: Intercalation of hexacyanoferrate(III) ions. *J. Phys. Chem. B* **2005**, *109* (1), 389−393.
(33) Iyi, N.; Fujii, K.; Okamoto, K.; Sasaki, T. Factors influencing the hydration of layered double hydroxides (LDHs) and the appearance of an intermediate second staging phase. *Appl. Clay Sci.* **2007**, *35* (3-4), 218−227.
(34) Aimoz, L.; Taviot-Gueho, C.; Churakov, S. V.; Chukalina, M.; Dahn, R.; Curti, E.; Bordet, P.; Vespa, M. Anion and cation order in iodide-bearing Mg/Zn-Al layered double hydroxides. *J. Phys. Chem. C* **2012**, *116* (9), 5460−5475.
(35) Jobbagy, M.; Iyi, N. Interplay of charge density and relative humidity on the structure of nitrate layered double hydroxides. *J. Phys. Chem. C* **2010**, *114* (42), 18153−18158.
(36) Prasanna, S. V.; Radha, A. V.; Kamath, P. V.; Kannan, S. Bromide-ion distribution in the interlayer of the layered double hydroxides of Zn and Al: Observation of positional disorder. *Clays Clay Miner.* **2009**, *57* (1), 82−92.
(37) Bastianini, M.; Costenaro, D.; Bisio, C.; Marchese, L.; Costantino, U.; Vivani, R.; Nocchetti, M. On the intercalation of the iodine−iodide couple on layered double hydroxides with different particle sizes. *Inorg. Chem.* **2012**, *51* (4), 2560−2568.
(38) Sposito, G. *The Thermodynamics of Soil Solutions*; Oxford Science Publ.: Oxford, U.K., 1981.

(39) Nagendran, S.; Kamath, P. V. Structure of the chloride- and bromide-intercalated layered double hydroxides of Li and Al. Interplay of Coulombic and hydrogen-bonding interactions in the interlayer gallery. *Eur. J. Inorg. Chem.* **2013**, *2013* (26), 4686−4693.
(40) Hines, D. R.; Solin, S. A.; Costantino, U.; Nocchetti, M. Physical properties of fixed-charge layer double hydroxides. *Phys. Rev. B* **2000**, *61*, 11348−11358.
(41) Kalinichev, A. G.; Kirkpatrick, R. J. Molecular dynamics modeling of chloride binding to the surfaces of calcium hydroxide, hydrated calcium aluminate, and calcium silicate phases. *Chem. Mater.* **2002**, *14* (8), 3539−3549.
(42) Kalinichev, A. G.; Kirkpatrick, R. J.; Cygan, R. T. Molecular modeling of the structure and dynamics of the interlayer and surface species of mixed-metal layered hydroxides: Chloride and water in hydrocalumite (Friedel's salt). *Am. Mineral.* **2000**, *85* (7-8), 1046−1052.
(43) Thomas, G. S.; Kamath, P. V.; Kannan, S. Variable temperature PXRD studies of $LiAl_2(OH)_6X.H_2O$ (X = Cl, Br): Observation of disorder → order transformation in the interlayer. *J. Phys. Chem. C* **2007**, *111* (51), 18980−18984.
(44) Li, H.; Ma, J.; Evans, D. G.; Zhou, T.; Li, F.; Duan, X. Molecular dynamics modeling of the structures and binding energies of alpha-nickel hydroxides and nickel−aluminum layered double hydroxides containing various interlayer guest anions. *Chem. Mater.* **2006**, *18* (18), 4405−4414.
(45) Gaines, G. L.; Thomas, H. C. Adsorption studies on clay minerals. II. A formulation of the thermodynamics of exchange adsorption. *J. Chem. Phys.* **1953**, *21* (4), 714−718.
(46) Cavani, F.; Trifiro, F.; Vaccari, A. Hydrotalcite-type anionic clays: Preparation, properties and applications. *Catal. Today* **1991**, *11* (2), 173−301.
(47) Bravo-Suárez, J. J.; Paez-Mozo, E. A.; Oyama, S. T. Models for the estimation of thermodynamic properties of layered double hydroxides: Application to the study of their anion exchange characteristics. *Quim. Nova* **2004**, *27* (4), 574−581.
(48) Barrer, R. M.; Townsend, R. P. Transition-metal ion exchange in zeolites. 2. Amines of Co^{2+}, Cu^{2+} and Zn^{2+} in clinoptilolite, mordenite and phillpsite. *J. Chem. Soc., Faraday Trans. 1* **1976**, *72*, 2650−2660.
(49) Barrer, R. M.; Klinowski, J. Influence of framework charge density on ion-exchange properties of zeolites. *J. Chem. Soc., Faraday Trans. 1* **1972**, *68*, 1956−1963.
(50) Shannon, R. D. Revised effective ionic radii and systematic studies of interatomic distances in halides and chalcogenides. *Acta Crystallogr. Sect. B.* **1976**, *32*, 751−767.
(51) Eisenman, G. Cation selective glass electrodes and their mode of operation. *Biophys. J.* **1962**, *2*, 259−323.
(52) Xu, Z. P.; Zeng, H. C. Abrupt structural transformation in hydrotalcite-like compounds $Mg_{1-x}Al_x(OH)_2(NO_3)_x \cdot nH_2O$ as a continuous function of nitrate anions. *J. Phys. Chem. B* **2001**, *105* (9), 1743−1749.
(53) Richardson, I. G. Clarification of possible ordered distributions of trivalent cations in layered double hydroxides and an explanation for the observed variation in the lower solid-solution limit. *Acta Crystallogr., Sect. B* **2013**, *69* (6), 629−633.